J Am Oil Chem Soc (2009) 86:1141–1147
DOI 10.1007/s11746-009-1457-5

ORIGINAL PAPER

Catalytic Activity of Ruthenium Nanoparticles Supported on Carbon Nanotubes for Hydrogenation of Soybean Oil

Shanshan Guo · Kong Yong Liew · Jinlin Li

Received: 17 November 2008 / Revised: 30 June 2009 / Accepted: 22 July 2009 / Published online: 20 August 2009

Abstract Ruthenium catalysts supported on multiwalled carbon nanotubes (MCNTs) with different loadings (1% wt, 3% wt, 5% wt) were prepared by reduction with H_2 or $NaBH_4$ for selective hydrogenation of soybean oil at 338 K and initial pressure of 1.066 MPa. These catalysts were characterized using transmission electron microscopy (TEM), X-ray powder diffraction (XRD), N_2 adsorption–desorption, and H_2-temperature programmed desorption (TPD) techniques. Ru particles were dispersed more homogeneously on the surface of the nanotubes after being reduced with H_2 than with $NaBH_4$. The catalysts with 3% and 5% Ru loadings had higher hydrogenation activity. The $NaBH_4$-reduced catalyst had higher *cis*-isomer selectivity.

Keywords Ru · $NaBH_4$ · H_2 · Hydrogenation · Soybean oil · Activity

Introduction

Vegetable oils are complex mixtures of triglycerides of fatty acids with up to 22 carbon atoms which may have zero to three double bonds in each of the fatty-acid chains [1]. The aim of partial hydrogenation is to decrease the amount of polyunsaturates while avoiding formation of saturates and *trans* products. In recent years, the negative health effects of *trans* fats have received increasing attention and they are considered to be even more detrimental than saturated fats [2]. Thus, it is important to produce hydrogenated edible oils with low *trans*-isomer content.

Carbon materials are widely used as supports for hydrogenation catalysts due to the fact that carbon has valuable characteristics not possessed by other supports. Carbon nanotubes, either single or multiwalled, have been widely used as supports for selective hydrogenation reactions because of their large surface areas, stability, and inertness [3–5]. Their surface can also be modified to incorporate various functional groups which can complex with ionic species or molecules as active sites for a variety of specific reactions. Furthermore, the uniform mesopores in carbon nanotubes may also serve as nanoreactors for shape- and size-selective reactions. The catalysts used in commercial hydrogenation are usually Ni supported on silica or alumina. Noble-metal catalysts are not often used due to their high cost. However, it was previously demonstrated that, under certain conditions, the Ru(II) catalyst has improved activity and *cis* selectivity compared with traditional heterogeneous Ni catalysts [6, 7]. Use of Ru as a hydrogenation catalyst has been reported [8, 9]; however, no reports have been published on the activity and selectivity in hydrogenation of vegetable oils with Ru^0 catalysts loaded onto MCNTs.

The present work reports the preparation and characterization of Ru-supported MCNT catalysts and the implications of their use in hydrogenation reactions. The catalytic properties were investigated in selective hydrogenation of soybean oil under mild reaction conditions. The support and Ru catalysts were characterized using transmission electron microscopy (TEM), temperature programmed desorption (H_2-TPD), X-ray powder diffraction (XRD), and N_2 adsorption–desorption. Hydrogenation of soybean oil was carried out at 338 K and initial pressure 1.066 MPa catalyzed by Ru catalyst supported on MCNTs.

S. Guo · K. Y. Liew · J. Li (✉)
Key Laboratory of Catalysis and Materials Science,
State Ethnic Affairs Commission and Ministry of Education,
South-Central University for Nationalities,
430074 Wuhan, China
e-mail: jinlinli@hotmail.com; lij@mail.scuec.edu.cn

Experimental

Catalyst Preparation

The multiwalled carbon nanotubes (MCNTs) were supplied by Chengdu Organic Chemicals Company Ltd., China. The surface area, average pore diameter, and pore volume of the MCNTs are 184.8 m^2/g, 2.7 nm, and 2.237 cm^3/g, respectively. MCNTs were purified by concentrated nitric acid treatment at 383 K for 4 h in order to remove residual impurities and develop oxygen-containing surface groups, which act as anchoring sites for the precursor metal to be impregnated. The solid was filtered and washed several times with distilled water until pH reached 7 and then dried overnight at 383 K.

Two series of Ru/MCNTs catalysts with different loadings of metal were prepared by different reduction methods. An appropriate amount of Ru salt [$Ru(NO)(NO_3)_3$, 31.3% Ru, Alfa Aesar] was dissolved in 10 mL distilled water, then the carbon nanotubes (0.7 g) were added and ultrasonicated for 1 h. In one series, after evaporation of the solvent, the samples were dried at room temperature for 12 h and then at 383 K for 12 h before reduction at 673 K by H_2 for 6 h; the catalysts prepared are denoted by 1% Ru/MCNTs–H_2 (a), 3% Ru/MCNTs–H_2 (b), and 5% Ru/MCNTs–H_2 (c). In another series, 50 mL $NaBH_4$ solution (0.05 mol L^{-1}) was added to the flask containing the impregnated Ru catalyst, the contents of which were filtered after stirring for 0.5 h and the residue was washed with a large amount of distilled water, dried at 383 K in a vacuum oven for 12 h, and denoted by 1% Ru/MCNTs–$NaBH_4$ (d), 3% Ru/MCNTs–$NaBH_4$ (e), and 5% Ru/MCNTs–$NaBH_4$ (f). Ru content in the catalysts was determined by inductively coupled plasma atomic emission spectroscopy (ICP-AES) with accuracy of ±0.1 wt.% Ru.

Catalyst Characterization

Transmission Electron Microscopy

TEM is a conventional method used to give detailed information about the shape, mean size, and size distribution of metallic dispersions. The microstructure of the carbon nanotubes supporting the Ru material was observed by FEI Tecnai G220 microscope operated at accelerating voltage of 200 kV. The average size and distribution of ruthenium particles were obtained from the diameter of more than 250 Ru black spots.

X-ray Diffraction

Powder X-ray diffraction (XRD) measurements were carried out on a Brukers D8 powder X-ray diffractometer, using Cu K_α radiation ($\lambda = 1.54056$ Å) at 40 kV and 40 mA. Diffraction intensities were recorded from 20° to 80° at scan rate of 4°/min with step size of 0.016°/step.

N_2 Adsorption–Desorption Measurements

N_2 adsorption–desorption was carried out with a Quantachrome Autosorb-1 surface area and pore size analyzer at 77 K. The samples were first degassed at 473 K for 6 h. The surface areas of samples were obtained using N_2 adsorption isotherm with the Brunauer–Emmett–Teller (BET) equation. The average pore diameters were calculated by the Barrett-Joyner-Halenda method from the desorption branch.

Hydrogen Temperature Programmed Desorption (H_2-TPD)

H_2 chemisorption was measured with H_2-TPD using a Zeton Altamira AMI-200 system. After reduction, the catalyst was pretreated in H_2 at 673 K for 2 h and cooled under flowing H_2 to 373 K, then held at 373 K under flowing Ar to remove physisorbed or weakly bound species prior to increasing the temperature slowly to the reduction temperature. At that temperature, the catalysts were held under flowing Ar to desorb the remaining chemisorbed H_2. The TPD spectra were integrated and the number of moles of desorbed H_2 was determined by comparing the area of calibration pulses of H_2 in Ar.

Hydrogenation of Soybean Oil

Hydrogenation of soybean oil was performed at 338 K in a continuously stirred slurry reactor (CSTR, 150 ml) with stirring rate of 1,000 rpm. The ruthenium catalysts (0.2 g) and 0.045 mol soybean oil (total volume 50 ml) were added to the reactor. The reactor was purged five times with hydrogen to remove residual air. The reaction began with initial pressure of 1.066 MPa (about 0.038 mol H_2) at 338 K with continuous stirring. An electro-manometer measured the hydrogen consumption while a computer recorded the data. The reaction stopped after the hydrogen was completely consumed.

The fatty-acid composition of the hydrogenated soybean oil products was analyzed using an Agilent 6890-5973 GC-MS with HP-1 column after the samples were converted into their methyl esters according to a reported method [10]. The column temperature was programmed from 373 to 523 K at 5 K min^{-1} with nitrogen as the carrier gas. The injection and detection temperatures were set at 493 and 523 K, respectively. Palmitic acid served as the internal standard.

For the quantitative determination of the *cis–trans* isomer ratio [1], the methyl esters obtained were dried under an N_2 atmosphere and then injected into a liquid Fourier-

transform infrared (FTIR) ZnSe cell using a Nicolet 470 spectrometer equipped with a computer. The IR spectra at 2 cm^{-1} resolutions in the range from 3,200 to 800 cm^{-1} with 32 scans were collected. The peak areas centered at 3,006 cm^{-1} corresponding to the *cis* configuration in oleic acid and at 966 cm^{-1} corresponding to the *trans* form in elaidic acid were measured and plotted against the respective acid concentrations. The concentrations of these isomers in each of the sample were obtained from the calibration plots and normalized to 100%.

Results and Discussion

XRD

Figure 1 shows the XRD patterns of pristine MCNTs and their corresponding Ru-supported MCNTs. Characteristic diffraction peaks of graphite can be seen at 26.5°, 42.7°, and 53.6°, assigned to the graphite crystallographic planes (002), (100), and (004), respectively. No Ru peak is detected as the amount of Ru is insufficient to show diffraction peaks or because the Ru particles were well dispersed on the surface of the MCNTs as shown in the TEM micrographs. However, as the amount of Ru increased, the graphite peak intensity decreased, which may be caused by the gradual destruction of the periodicity between the graphene layers and within the layer [11].

Particle Size Distribution and Influence of Particle Size

Typical TEM micrographs and size distribution histograms of the six prepared samples are shown in Fig. 2. The Ru particles are of nanometer size with average diameters of

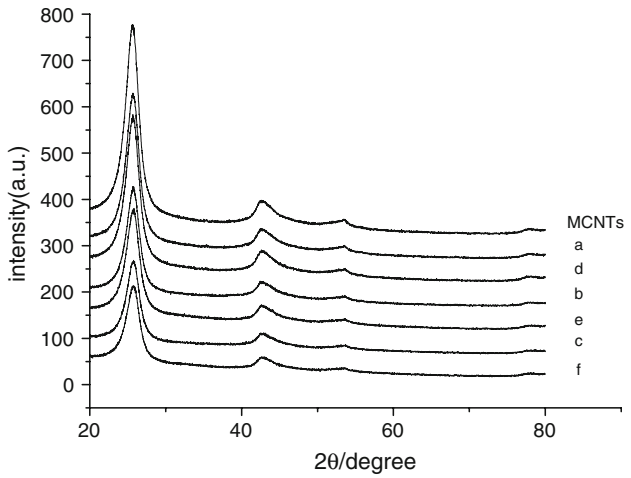

Fig. 1 XRD profiles: *a* 1% Ru/MCNTs–H_2, *b* 3% Ru/MCNTs–H_2, *c* 5% Ru/MCNTs–H_2, *d* 1% Ru/MCNTs–$NaBH_4$, *e* 3% Ru/MCNTs–$NaBH_4$, and *f* 5% Ru/MCNTs–$NaBH_4$

1.3 ± 0.4, 2.5 ± 0.7, 1.8 ± 0.4, 2.8 ± 1.3, 3.7 ± 1.4, and 2.5 ± 1.1 nm. From Fig. 2a–c, it can be seen that most of the Ru particles on Ru/CNTs–H_2 are dispersed homogeneously on the outer surface of the nanotubes. From Fig. 2d, e, it is observed that the ruthenium particles reduced by $NaBH_4$ were aggregated and hence larger than the particles reduced by H_2. Initially, the size of the particles formed using $NaBH_4$ was small; simultaneously, a large number of Ru^{3+} was reduced to Ru^0 rapidly. Some of the particles aggregated, resulting in larger particles and wide particle size distributions [12]. From the TEM data, the particle size increases from 1% to 3% Ru content and then decreases when passing from 3% to 5% Ru content. This can be explained qualitatively as follows: At low Ru concentration (1% Ru catalyst), the size of the metal particles formed both inside and outside the carbon nanotubes was small. As the Ru concentration was increased to 3% Ru, more particles were formed inside as well as outside the tubes, initially small but then growing larger, which may then plug the openings of the tubes. At higher Ru concentration (5% Ru catalyst), the larger metal particles that formed plugged the openings of the nanotubes, obstructing further growth of the particles inside the tubes, so only particles outside the tubes grew larger, resulting in a wide particle size distribution and a decrease in the average particle size. Thus, seriously aggregated particles in the catalysts reduced by $NaBH_4$ also affected the average particle size, as shown by the TEM micrographs and the histograms.

Surface Properties

Information on the surface area and pore volume of the catalysts was obtained from the N_2 adsorption isotherms and is shown in Table 1. The pore volume of raw adsorption after loading with Ru indicates that a fraction of the pores was obstructed by MCNTs: 3.109 $cm^3\ g^{-1}$, decreasing to 2.237 $cm^3\ g^{-1}$ after treatment with concentrated nitric acid, perhaps attributable to the various functional groups such as carboxyl (–COOH), hydroxyl (–OH), and carbonyl (–C=O) [13]. Kuznetsova et al. [14] pointed out that functional groups, when present on the nanotubes, block the adsorption of gases and severely diminish their adsorption capacity. The decreased adsorption after loading with Ru indicates that a fraction of the pores was obstructed by the deposited Ru particles, excluding a fraction of micropores with width less than 2.7 nm [15].

H_2-TPD

The amounts of H_2 desorption of the catalysts are listed in Table 1. There is only one H_2 desorption peak in the catalysts and their supports. Interestingly, the amount of H_2

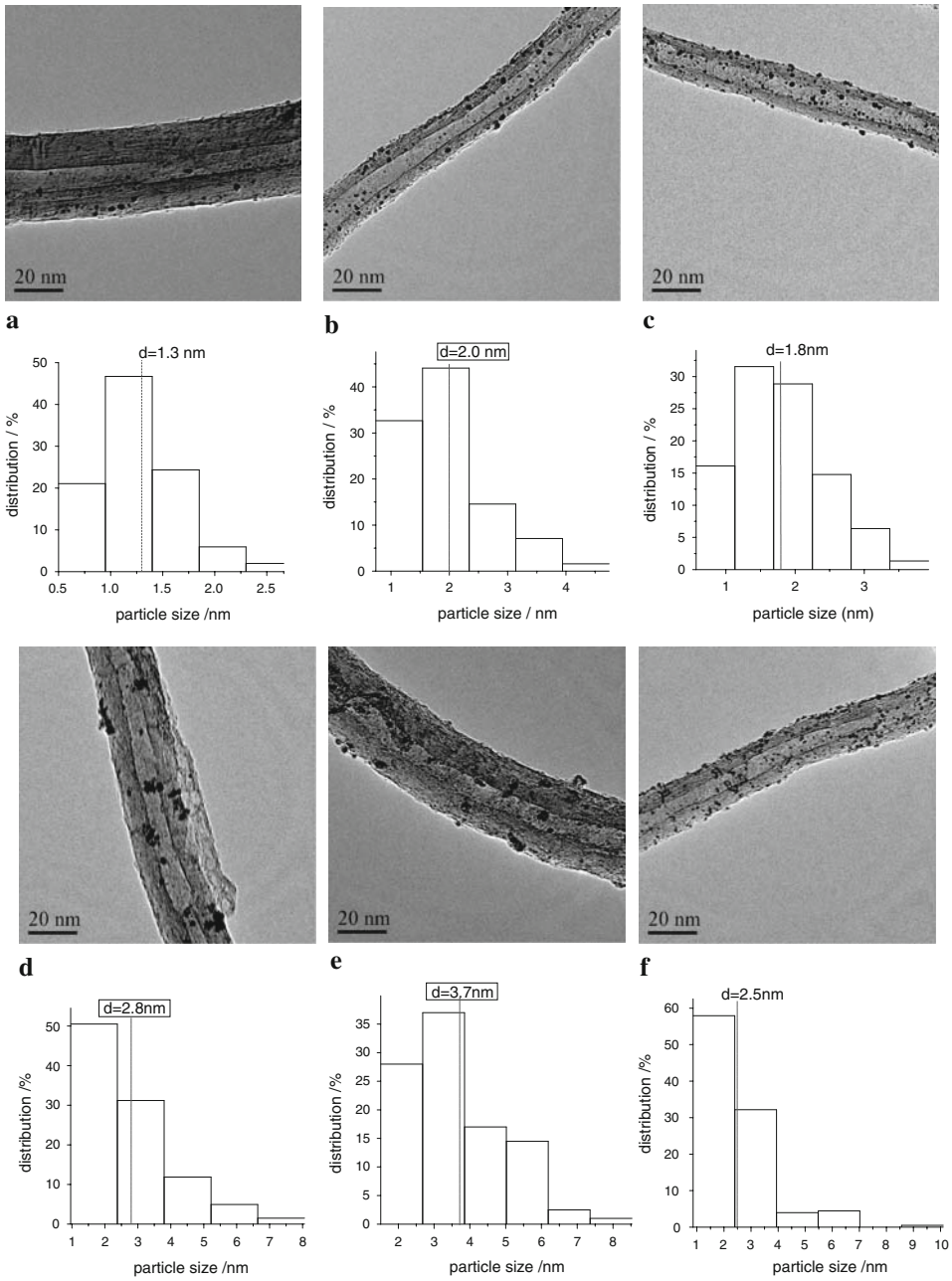

Fig. 2 TEM images (*above*) and particle sizes distributions (*below*) of: **a** 1% Ru/MCNTs–H_2, **b** 3% Ru/MCNTs–H_2, **c** 5% Ru/MCNTs–H_2, **d** 1% Ru/MCNTs–$NaBH_4$, **e** 3% Ru/MCNTs–$NaBH_4$, and **f** 5% Ru/MCNTs–$NaBH_4$

desorption on 3% Ru/MCNTs–H_2 (b) and 3% Ru/MCNTs–$NaBH_4$ (e) is larger than that in the other samples. The high activity of 3% Ru/MCNTs–H_2 (b) and 3% Ru/MCNTs–$NaBH_4$ (e) for hydrogenation (described in the next section) can thus be explained, since the first step in the process of hydrogenation is simultaneous adsorption of the H_2 molecule and carbon–carbon double bonds.

Hydrogenation of Soybean Oil

The rate of hydrogenation of soybean oil was measured by the hydrogen consumption at 338 K and initial pressure of 1.066 MPa. As shown in Fig. 3, the hydrogen consumption for all the catalysts increased nearly linearly initially, after which the rate decreased as the fatty acids with multiple double bonds were depleted. Finally, the rate of reaction decreased further as fatty acids with one double bond were hydrogenated. The activity of the catalysts is in the order 3% Ru $\cong$ 5% Ru $>$ 1% Ru in both series. The 3% Ru and 5% Ru catalysts have similar activity, although the total amounts of Ru present are quite different. In terms of amount of Ru, the 3% Ru catalysts should have the highest activity (curves c and d). This is not surprising since the H_2 uptakes by these catalysts were the highest as determined by TPD. The turnover frequency (TOF) of hydrogen consumption, defined as moles of H_2 consumed per moles of

Table 1 Surface area, pore volume, and pore diameter calculated from N_2 adsorption–desorption for catalysts: (a) 1% Ru/MCNTs–H_2, (b) 3% Ru/MCNTs–H_2, (c) 5% Ru/MCNTs–H_2, (d) 1% Ru/MCNTs–$NaBH_4$, (e) 3% Ru/MCNTs–$NaBH_4$, and (f) 5% Ru/MCNTs–$NaBH_4$

Catalysts	Surface area ($m^2\ g^{-1}$)	Pore volume ($cm^3\ g^{-1}$)	Pore diameter (nm)	H_2 desorption ($\mu mol\ g_{cat}^{-1}$)
Raw MCNTs	185.1	3.109	2.7	/
Treated MCNTs	184.8	2.237	2.7	0
a	191.9	2.014	2.7	81.6
b	220.3	2.058	2.7	151.8
c	209.6	1.891	2.7	130.8
d	169.1	2.000	2.7	103.5
e	154.9	1.862	2.7	161
f	168.3	1.942	2.7	152.1

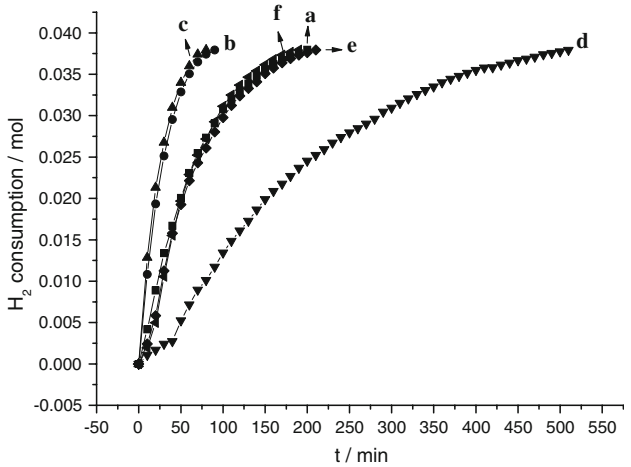

Fig. 3 Hydrogen consumption of soybean oil with supported Ru as a catalyst as a function of time. Reaction conditions: soybean oil 0.045 mol; Ru catalysts 0.1 g; initial pressure 1.066 MPa; temperature 338 K. *a* 1% Ru/MCNTs–H_2, *b* 3% Ru/MCNTs–H_2, *c* 5% Ru/MCNTs–H_2, *d* 1% Ru/MCNTs–$NaBH_4$, *e* 3% Ru/MCNTs–$NaBH_4$, and *f* 5% Ru/MCNTs–$NaBH_4$

Ru^0 sites per second, was calculated by the following equation:

$$\mathrm{TOF}\,(s^{-1}) = \frac{N_{H_2}}{\frac{w_{catal}\times wt\%}{Ar(Ru)} \times t \times 60},$$

where N_{H_2} is number of moles of H_2 consumed, wt% is the Ru^0 loading of the catalysts, w_{catal} is the dosage of catalysts in the reaction, and Ar(Ru) is the atomic weight of Ru^0 (Table 2).

It is observed that the activity in terms of TOF decreases from 1% Ru to 3% Ru due to the increase in particle size resulting in a smaller proportion of exposed surface of Ru atoms available to catalyze the reaction, while the decreased TOF from 3% Ru to 5% Ru, despite the latter having a smaller average particle size than the former, is due to the inaccessibility of the Ru atoms inside the nanotubes. This trend is true for both series of catalysts.

Table 2 TOF of Ru/MCNTs: (a) 1% Ru/MCNTs–H_2, (b) 3% Ru/MCNTs–H_2, (c) 5% Ru/MCNTs–H_2, (d) 1% Ru/MCNTs–$NaBH_4$, (e) 3% Ru/MCNTs–$NaBH_4$, and (f) 5% Ru/MCNTs–$NaBH_4$

Catalyst	a	b	c	d	e	f
TOF (s^{-1})	0.1596	0.1182	0.0798	0.0626	0.0507	0.0336

Selectivity of Hydrogenation Reaction

The hydrogenation of edible oil is generally depicted as follows:

$$\mathrm{Linolenic\ (LL)} + H_2 \xrightarrow{k_1} \mathrm{linoleic\ (L)} + H_2 \xrightarrow{k_2} \mathrm{oleic\ (O)} + H_2 \xrightarrow{k_3} \mathrm{stearic\ (S)}. \quad (1)$$

Table 3 shows the iodine value (IV) and fatty-acid composition of soybean oil and hydrogenated soybean oil with different catalysts. The iodine value (IV) shows that there are no large differences between each sample after hydrogenation, because the hydrogen consumption of each sample is nearly the same.

The hydrogen was consumed mainly by the C18:3, C18:2, and C18:1 acid moieties. Thus, on hydrogenation, the concentrations of C18:3 and C18:2 decreased while the C18:1 and C18:0 increased, and there was no C18:3 after the reaction. Comparing the increase in concentration of the saturated fatty acid C18:0 and the mono-unsaturated acid C18:1, the rate of hydrogenation of C18:2 is faster than that of C18:1. It is generally accepted that hydrogenation occurs via the half-hydrogenated state for most hydrogenations [16]. Hence, once the unsaturated double bond is adsorbed on the active sites of Ru nanoparticles, it will then react with an adjacent adsorbed hydrogen atom to form an unstable complex with a partially hydrogenated double bond. This unstable complex may or may not desorb from the Ru nanoparticle surface and being hydrogenated to a single bond by reacting with another hydrogen

Table 3 Iodine value (IV) and fatty-acid composition of soybean oil and hydrogenated soybean oil with different catalysts: (a) 1% Ru/MCNTs–H_2, (b) 3% Ru/MCNTs–H_2, (c) 5% Ru/MCNTs–H_2, (d) 1% Ru/MCNTs–$NaBH_4$, (e) 3% Ru/MCNTs–$NaBH_4$, and (f) 5% Ru/MCNTs–$NaBH_4$

	IV	Fatty-acid composition (percentage of fatty acid)									*% cis*
		C16:0	C16:1	C18:0	C18:1	C18:2	C18:3	C20:0	C20:1	C22:0	
Oil	113	11.3	0.2	5.0	33.8	47.3	1.0	0.8	0.2	0.4	100
a	66	11.3	0.2	46.1	35.6	4.5	0	1.0	0	0.4	73.3
b	58	11.3	0.2	42.7	36.1	7.3	0	1.0	0	0.4	72.6
c	63	11.3	0.2	43.4	36.5	6.2	0	1.0	0	0.4	72.3
d	71	11.3	0.2	39.7	38.1	8.3	0	1.0	0	0.4	77.8
e	55	11.3	0.2	44.6	33.6	7.9	0	1.0	0	0.4	75.4
f	64	11.3	0.2	44.4	33.8	7.8	0	1.0	0	0.4	80.9

atom [1]; meanwhile the remaining double bond will be isomerized to the *trans* isomer, which is more thermodynamically stable than the *cis* isomer.

cis–trans Isomerization

The formation of *trans* isomers of the remaining unsaturated fatty acids is to be avoided as far as possible for edible oils and fats as they are unhealthy for consumption. Nearly all of the double bonds in the refined soybean oil are in the *cis* configuration, which exhibits a distinct infrared (IR) band at $\sim$3,006 cm^{-1} (*cis*). After hydrogenation, the peak intensity of the *trans* isomer, as elaidic acid, increased at 966 cm^{-1} (*trans*). Table 3 shows that, after hydrogenation, C18:2 and C18:1 were the main unsaturated contents, so that the ratio of *cis* and *trans* composition for C18:1 and C18:2 can be approximated by the IR results. The results are shown in Table 3, which shows that the *cis* configuration of the products decreased to 72–80% after hydrogenation, but remains high. Compared with the catalysts reduced by hydrogen, the catalysts reduced by $NaBH_4$ resulted in a higher *cis*-isomer content with a smaller portion of double bonds converted to *trans* configuration. This result is perplexing as the latter series of catalysts has lower activity for hydrogenation than the former and catalysts with higher activity generally lead to lower level of *cis–trans* isomerization. The remain differences between the two series of catalysts are that the exposed Ru particle sizes of the $NaBH_4$-reduced catalysts are larger than those reduced by H_2 and secondly the former may be contaminated by traces of Na^+ and B. The differences in particle size may have an effect on the *cis–trans* isomerization which accompanies the hydrogenation reaction requiring the simultaneous adsorption of both hydrogen and double bond on adjacent sites. However, as even particles with the mean size of 1.3 nm in 1% Ru/MCNTs should be large enough to accommodate this simultaneous adsorption, we can thus rule out the size effect as the major factor affecting the *cis–trans* selectivity. It is known that some adsorbed molecules such as amines could reduce the *trans* formation during hydrogenation [17]. Thus, the presence of trace amounts of Na^+ or B contaminants on the catalysts may have affected the *cis–trans* selectivity. However, much work needs to be done to confirm this conjecture.

In summary, as far as we are aware, this is the first time that carbon nanotubes have been used as a support for Ru as a catalyst for hydrogenation of oils and fats. The active site for hydrogenation is in no doubt the Ru metal, the activity of which is lower than that of unsupported nanosized Pd or Pt [18] but much higher than that of supported conventional Ni catalyst. However, the *cis–trans* selectivity, which is comparable to that of Pd and Pt and much more *cis*-selective than that of conventional Ni as a catalyst, is found to be tunable by the presence of trace amounts of inorganic contaminants or due to the reaction proceeding inside the mesopores. This is being investigated.

Acknowledgments Financial support by the National Natural Science Foundation of China (grant nos. 20473114 and 20590360) is gratefully acknowledged.

References

1. Choo HP, Liew KY, Liu H, Seng CE, Mahmood WAK, Bettahar M (2003) Activity and selectivity of noble metal colloids for the hydrogenation of polyunsaturated soybean oil. J Mol Catal A 191:113–121
2. Oomen CM, Ocke MC, Feskens EJM, van Erp-Baart M-A, Kok FJ, Kromhout D (2001) Association between *trans* fatty acid intake and 10-year risk of coronary heart disease in the Zutphen Elderly Study: a prospective population-based study. Lancet 357(9258):746–751
3. Planeix JM, Coustel N, Coq B, Brotons V, Kumbhar PS, Dutartre R et al (1994) Application of carbon nanotubes as supports in heterogeneous catalysis. J Am Chem Soc 116:7935–7936
4. Lordi V, Yao N, Wei J (2001) Method for supporting platinum on single-walled carbon nanotubes for a selective hydrogenation catalysts. Chem Mater 13:733–737
5. Brotons V, Coq B, Planeix JM (1997) Catalytic influence of bimetallic phases for the synthesis of single-walled carbon nanotubes. J Mol Catal A 116:397–403

6. Bello C, Diosady LL, Graydon WF, Rubin LJ (1985) Homogeneous catalytic hydrogenation of canola oil using a ruthenium catalyst. J Am Oil Chem Soc 62:1587–1592
7. Diosady LL, Graydon WF, Koseoglu SS, Rubin LJ (1984) Hydrogenation of canola oil in the presence of arene chrome carbonyl complexes. Can Inst Food Sci Technol J 17:216–223
8. Mendes MJ, Santos OAA, Jordão E, Silva AM (2001) Hydrogenation of oleic acid over ruthenium catalysts. Appl Catal A 217:253–262
9. Maris EP, Davis RJ (2007) Hydrogenolysis of glycerol over carbon-supported Ru and Pt catalysts. J Catal 249:328–337
10. Anon (1995) Palm oil test methods. Palm Oil Research Institute Malaysia, Bangi, p 83
11. Ovejero G, Sotelo JL, Romero MD, Rodríguez A, Ocaña MA, Rodríguez G, García J (2006) Multiwalled carbon nanotubes for liquid-phase oxidation, functionalization, characterization and catalytic activity. Ind Eng Chem Res 45:2206–2212
12. Xu B, Liew KY, Li J (2007) Effect of Ru nanoparticle size on hydrogenation of soybean oil. J Am Oil Chem Soc 84:117–122
13. Ebbesen TW, Hiura H, Bisher ME, Treacy MMJ, Shreeve-Keyer JL, Haushalter RC (1996) Decoration of carbon nanotubes. Adv Mater 8:155–157
14. Kuznetsova A, Mawhinney DB, Naumenko V, Yates JT, Liu J, Smalley RE (2000) Enhancement of adsorption inside of single-walled nanotubes: opening the entry ports. Chem Phys Lett 321:292–296
15. Lia CH, Yua ZX, Yaoa KF, Jib SF, Lianga Ji (2005) Nitrobenzene hydrogenation with carbon nanotube-supported platinum catalyst under mild conditions. J Mol Catal A 226:101–105
16. Rase HF (2000) Handbook of commercial catalysts. CRC, New York, pp 182–194
17. Nohair B, Especel C, Marécot P, Montassier C, Hoang LC, Barbier J (2004) Selective hydrogenation of sunflower oil over supported precious metals. Comptes Rend Chim 7:113–118
18. Choo HP, Liew KY, Liu HF, Seng CE (2001) Hydrogenation of palm olein catalyzed by polymer stabilized Pt colloids. J Mol Catal A Chem 165:127–134